Letters

A Modified Y-Source DC–DC Converter With High Voltage-Gains and Low Switch Stresses

Jing Yuan, *Student Member, IEEE*, Ali Mostaan, Yongheng Yang, *Senior Member, IEEE*, Yam P. Siwakoti, *Senior Member, IEEE*, and Frede Blaabjerg, *Fellow, IEEE*

***Abstract*—This letter proposes a modified Y-source dc–dc converter, which features higher voltage-gains but lower voltage stresses on the components. Moreover, the proposed converter draws a continuous current from the dc input with much control flexibility (i.e., a wide range of adjustable duty cycles). Additionally, the coupled inductors have a low turns ratio, and the core saturation issue is avoided due to the dc-current-blocking capacitor. A detailed analysis of the proposed converter is provided, and the performance is benchmarked with selected coupled-inductors-based converters on various aspects. Experimental tests confirm the theoretical analysis.**

***Index Terms*—DC-DC converter, renewable energy, voltage stress, Y-source converter.**

I. Introduction

DC–DC converters are essential in the grid-integration of PV systems, where a high voltage conversion gain is usually required. Many attempts have thus been made to address the issues associated with conventional high-gain dc–dc converters, e.g., low efficiency for high power applications and high voltage stresses on power devices. On the other hand, extensive topologies for high conversion gains have been introduced in the literature [1]–[3]. Although these converters have high voltage gains, the voltage stress on the power switches is high or equal to the output voltage that can deteriorate the efficiency. Moreover, the adjustable duty cycle range is very limited when requiring a high boost ratio. Finally, the discontinuous current inputs further hinder the applications in the renewable energy applications. Although some modified dc–dc converters have a wide duty cycle and low voltage stresses on the switches, more components are utilized, when compared with conventional topologies [4]–[6].

Manuscript received October 23, 2019; revised November 25, 2019 and December 29, 2019; accepted December 30, 2019. Date of publication January 5, 2020; date of current version April 22, 2020. This work was supported by the research project – Reliable Power Electronic based Power Systems (REPEPS) by THE VELUX FOUNDATIONS under Award Ref. No.: 00016591. *(Corresponding author: Yongheng Yang.)*

J. Yuan, Y. Yang, and F. Blaabjerg are with the Department of Energy Technology, Aalborg University, 9220 Aalborg, Denmark (e-mail: yua@et.aau.dk; yoy@et.aau.dk; fbl@et.aau.dk).

A. Mostaan is with the Electrical Engineering Department, University of Guilan, Rasht, Iran (e-mail: ali_8457@yahoo.com).

Y. P. Siwakoti is with the Faculty of Engineering and IT, University of Technology, Sydney, Ultimo, NSW 2007, Australia (e-mail: yam.siwakoti@uts.edu.au).

Color versions of one or more of the figures in this article are available online at http://ieeexplore.ieee.org.

Digital Object Identifier 10.1109/TPEL.2020.2964153

Nevertheless, since the introduction of impedance-source converters [7], a vast array of high-gain converters have been developed. It has been proven that the coupled-inductors-based impedance networks can achieve better performances in terms of high voltage-gains and low component-counts [8]–[15]. For instance, the Γ-source impedance networks [8], [9] are typical high-boosting representatives, where coupled-inductors with smaller turns ratios are employed. The Γ-source converter can not only draw a discontinuous current from the dc input but also its adjustable range of duty cycles is limited. Another example among the high voltage-gain impedance-source converters is Y-source-based. The Y-source networks also use lower turns ratio coupled-inductors while offering much flexibility to design the conversion gain [10]–[12]. Unfortunately, similar to the Γ-source networks, the duty cycle for the Y-source networks can only be adjusted in a limited range. Moreover, the switches in these converters are connected to the output voltage side, which leads to high voltage stresses on the switches. In all, either the state-of-the-art solutions are difficult to control (less control flexibility) or there are high stresses on the components.

In light of the above, a modified Y-source-based converter is proposed in this letter. Compared to the prior-art high-gain dc–dc converters, the proposed converter can achieve high voltage-gains with the employment of a low turns-ratio coupled-inductor. More importantly, it can maintain low voltage stresses on the components even for high-voltage applications, and thus contribute to the component selection of smaller power ratings (i.e., lower costs). This distinct feature is achieved by shifting the power device to the input-side with respect to the conventional Y-source converter. The rest of the letter is organized as follows. The operational principles of the proposed dc–dc converter are detailed in Section III, where it is also compared with selected topologies. Experimental tests are performed on a 250-W prototype and the results are provided in Section III, which verifies the theoretical analysis and the superiority of the proposed converter. Finally, concluding remarks are given in Section IV.

II. Proposed Modified Y-Source Converter

A. Operation Principle

The proposed Y-source converter is shown in Fig. 1, which includes an input inductor (L), an active switch (S), two diodes

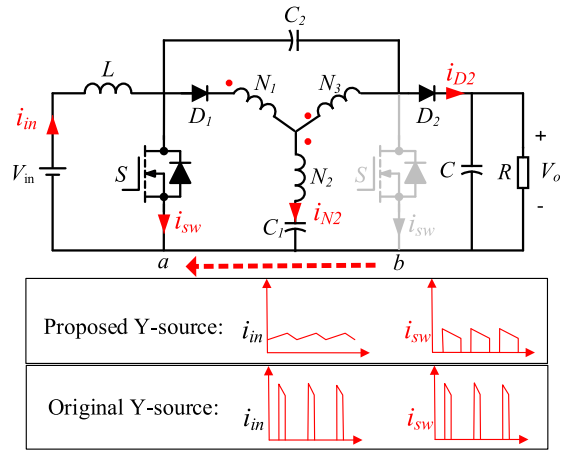

Fig. 1. Schematic of the proposed topology, showing that the power device is moved to the low-voltage side.

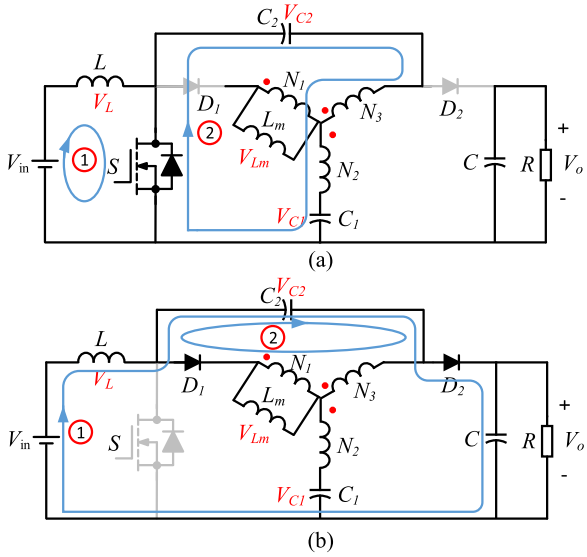

Fig. 2. Equivalent circuits of the proposed topology in: (a) ON-state and (b) OFF-state, where V_x represents the voltage on the component "x" and V_o is the output voltage.

(D_1, D_2), three capacitors (C_1, C_2, C), and a coupled-inductor with three windings (the turns ratios are denoted as N_1, N_2, and N_3). It can be observed in Fig. 1 that the position of the active switch is shifted from the high-voltage side to low-voltage side compared with the conventional Y-source dc–dc converter. In addition, the input current of the proposed converter is continuous and the peak switch current is reduced significantly. It is assumed that the power devices are ideal and the capacitor can maintain the output voltage as a constant. Then, the steady-state conditions of the converter can be analyzed. Clearly, there are two operation states (i.e., S is ON and OFF) in one switching cycle for the proposed converter, as shown in Fig. 2, where the magnetizing inductance is considered. Accordingly, the voltages across the inductor can be obtained as

$$V_{\mathrm{N1}} = V_{\mathrm{Lm}}, \quad V_{\mathrm{N2}} = \frac{N_2}{N_1} V_{\mathrm{Lm}}, \quad V_{\mathrm{N3}} = \frac{N_3}{N_1} V_{\mathrm{Lm}} \tag{1}$$

where V_{N1}, V_{N2}, V_{N3}, and V_{Lm} are the corresponding voltages on the windings N_1, N_2, N_3, and the magnetizing inductance L_m of the coupled-inductor.

As shown in Fig. 2(a), when S is turned ON, the input inductor L will be charged by the source, and accordingly, the inductor current increases linearly. Moreover, D_1 and D_2 are reverse-biased. Therefore, the capacitor C supplies the load R. According to the Kirchhoff's voltage law (KVL), it can be obtained that

$$V_L - V_{\mathrm{in}} = 0 \tag{2}$$

$$-V_{\mathrm{C2}} - V_{\mathrm{N3}} + V_{\mathrm{N2}} + V_{\mathrm{C1}} = 0 \tag{3}$$

in which V_{in} is the input voltage, V_L is the inductor voltage during the ON-state period, and V_{C1}, V_{C2} represent the capacitor voltage across C_1, C_2, respectively. Substituting (1) into (2) gives the voltage of the magnetizing inductance as

$$V_{\mathrm{Lm}} = \frac{N_1}{N_3 - N_2} \left(V_{\mathrm{C1}} - V_{\mathrm{C2}}\right). \tag{4}$$

When S is turned-OFF, see Fig. 2(b), the energy stored in the inductor L is released to the load through the impedance network. In this case, based on the KVL, the following equations can be obtained as

$$-V_L + V_{\mathrm{in}} + V_{\mathrm{C2}} - V_o = 0 \tag{5}$$

$$-V_{\mathrm{C2}} - V_{\mathrm{N3}} - V_{\mathrm{N1}} = 0. \tag{6}$$

Substituting (1) into (6) leads to the magnetizing voltage as

$$V_{\mathrm{Lm}} = -V_{\mathrm{C2}} \frac{N_1}{N_3 + N_1}. \tag{7}$$

By applying the voltage-second principle to the inductor L and L_m, i.e., (2), (4), (5), and (7), it can be obtained that

$$DV_{\mathrm{in}} + (1 - D)\left(V_{\mathrm{in}} + V_{\mathrm{C2}} - V_o\right) = 0 \tag{8}$$

$$D\frac{N_1\left(V_{\mathrm{C1}} - V_{\mathrm{C2}}\right)}{N_3 - N_2} + (1 - D)\left(-\frac{N_1}{N_1 + N_3} V_{\mathrm{C2}}\right) = 0 \tag{9}$$

with D being the duty cycle. Finally, the capacitor voltages and the voltage gain G can be expressed as

$$V_{\mathrm{C1}} = V_{\mathrm{in}} + V_{\mathrm{C2}} = \left(1 + \frac{KD}{1 - D}\right) V_{\mathrm{in}} \tag{10}$$

$$G = \frac{V_o}{V_{\mathrm{in}}} = \frac{1 + DK}{1 - D} \tag{11}$$

where the winding factor K is expressed as

$$K = \frac{N_3 + N_1}{N_3 - N_2}. \tag{12}$$

To ensure the voltage boosting, it is indicated in (12) that $N_3 > N_2$. The voltage gains for the proposed converter under different turns ratios and various duty cycles are shown in Fig. 3. It can be seen in Fig. 3 that the voltage gain becomes smaller when the turns ratio increases under the same duty cycle. In addition, the range of the duty cycle is much wider than that of the topologies in [8]–[12], as compared in Fig. 4.

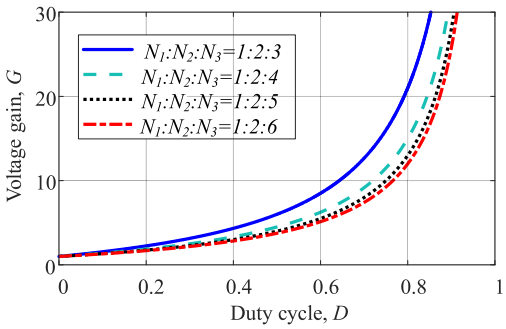

Fig. 3. Voltage gain of the proposed topology for different turns ratio.

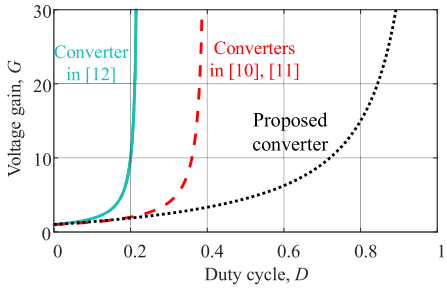

Fig. 4. Voltage gain of the proposed converter and selected converters for the same turns ratio.

B. Design Consideration

As the average capacitor current and the average magnetic inductor voltage are zero in one switching cycle. The average currents i_{N_1}, i_{N_2}, and i_{N_3} through winding the three windings are

$$i_{N_1} = \frac{N_3}{N_1} i_o, \quad i_{N_2} = 0, \quad i_{N_3} = i_o \tag{13}$$

where i_o is the output current. Based on the Kirchhoff's current law (KCL), it can be obtained that

$$i_{Lm} = i_{N_1} + i_{N_3} = \left(1 + \frac{N_3}{N_1}\right) i_o \tag{14}$$

with i_{Lm} being the magnetizing current. During the ON-state the magnetizing current flows to the winding N_1, and therefore, i_{N_2} and i_{N_3} are equal with together

$$i_{N_2(ON)} = i_{N_3(ON)}. \tag{15}$$

By using the ampere turn balance in the windings, we have

$$N_1 i_{N_1} + N_2 i_{N_2} = N_3 i_{N_3}. \tag{16}$$

Then, it can be obtained that

$$i_{N_2(ON)} = i_{N_3(ON)} = \frac{N_1}{N_3 - N_2} i_{N_1(ON)}. \tag{17}$$

In addition, i_{N_2} flows through C_1 and i_{N_3} flows through C_2, and thus the capacitors voltage ripples can be obtained as

$$\Delta v_{C_1} = \frac{N_1 i_{Lm}}{N_3 - N_2} \cdot \frac{D}{C_1 f}, \ \Delta v_{C_2} = \frac{N_1 i_{Lm}}{N_3 - N_2} \cdot \frac{D}{C_2 f} \tag{18}$$

in which f is the switching frequency. Therefore, the capacitor values can be calculated according to (18). Moreover, the output capacitor can be obtained as

$$C = \frac{i_o D}{\Delta v_C f} \tag{19}$$

where Δv_C is the voltage ripple of the output capacitor. The design of the coupled inductor is similar to the original Y-Source network [10], so the minimum value of the magnetizing inductance can be derived as

$$L_m = \frac{N_1 \left(V_{C2} - V_{C1}\right) D}{2 i_o \left(1 + \frac{N_3}{N_1}\right) \left(N_3 - N_2\right) f}. \tag{20}$$

C. Voltage Stress Analysis

To further assist the component selection, the voltage stresses over the active switch, diodes, and capacitors are analyzed. Notably, the voltage stress is defined as the ratio of the voltage across the corresponding component to the input voltage.

When S is OFF, the voltage $V_{\rm sw}$ across the switch can be obtained as

$$V_{\rm sw} = V_o - V_{\rm C2}. \tag{21}$$

By substituting (10) and (11) into (13), the voltage stress can be derived as

$$\frac{V_{\rm sw}}{V_{\rm in}} = \frac{G + K}{1 + K} = \frac{1}{1 - D}. \tag{22}$$

It is clear that the voltage stress of the switch is only determined by the duty cycle. When S is ON, the voltage stresses of the diodes can be obtained as

$$\frac{V_{d_1}}{V_o} = \frac{K^2 + KG + 2\,K}{1 + KD}, \ \frac{V_{\rm d_2}}{V_{\rm in}} = \frac{G + K}{1 + K}. \tag{23}$$

Based on the above, the suitable semiconductors can be chosen according to K and the required output voltage. Moreover, the capacitor stresses can be derived according to (10)

$$\frac{V_{\rm C1}}{V_{\rm in}} = \frac{KG + 1}{K + 1}, \ \frac{V_{\rm C2}}{V_{in}} = \frac{KG - K}{K + 1}. \tag{24}$$

D. Comparison With Selected Topologies

A comprehensive comparison between the proposed converter and selected topologies is summarized in Table I, where n is the turns ratio. It can be observed in Table I that the Γ-source converter has the lowest component-count among the benchmarked. However, the discontinuous input current is its main drawback. Although the modified Γ-source converter in [9] can draw a continuous input current, the duty cycle control range is narrow, as aforementioned. Compared to the Γ-source networks, the Y-source networks have a three-winding structure. The Y-source converter in [12] uses many components to achieve a higher voltage gain, which leads to an increased cost. Furthermore, although the converters in [10]–[12] have a better boost capability, the duty cycle is limited in a narrow range, which is also indicated in Fig. 4. This means that the control is very sensitive to the duty cycle, when a high voltage-gain is required. Although the converters in [4]–[6] have a wide duty cycle range, they have more components than the proposed converter. In addition, the input current ripple in [4] and [6] is high, which

TABLE I
BENCHMARKING OF SELECTED TOPOLOGIES BASED ON COUPLED INDUCTORS

Converters in	[4]	[5]	[6]	[8]	[9]	[10]	[11]	[12]	Proposed
Counts of inductors + coupled inductors	0+2	1+2	4+0	0+2	1+2	0+3	1+3	2+3	1+3
Counts of capacitors	4	5	1	2	3	2	3	5	3
Counts of switches	1	1	2	1	1	1	1	1	1
Counts of diodes	4	4	7	2	2	2	2	3	2
Input current ripple	high	low	high	high	low	high	low	low	low
Duty-cycle control range	$0<D<1$	$0<D<1$	$0<D<1$	$0<D<\frac{1}{1+\frac{1}{n-1}}$	$0<D<\frac{1}{2+\frac{1}{n-1}}$	$0<D<\frac{1}{K}$	$0<D<\frac{1}{K}$	$0<D<\frac{1}{K+2}$	$0<D<1$

n is the turns-ratio and K is coefficient defined in (12).

TABLE II
COMPARISON OF VOLTAGE STRESSES OVER THE COMPONENTS AMONG SELECTED Y-SOURCE CONVERTERS

Voltage stress	Y-source [10]	quasi-Y-source [11]	Proposed Y-source
C_1	$\frac{4G+1}{5}$	$\frac{4G+1}{5}$	$\frac{5G+1}{6}$
C_2	/	$\frac{4G-4}{5}$	$\frac{5G-5}{6}$
D_1	$4G$	$4G$	$\frac{4G+25}{6}$
D_2	G	G	$\frac{G+5}{6}$
S	G	G	$\frac{G+5}{6}$

TABLE III
DESIGN PARAMETERS OF THE PROPOSED CONVERTER

Parameter/Description	Value/Part Number
Rated Power	250 W
Input/Output Voltage	40/400 V
Capacitor/Input Inductor	100 μF/640 μH
Turns-Ratio	20:12:20
Core	B66397G0000X197
Switching Frequency	100 kHz
Duty Cycle	0.60
Switch S	IPP60R099C6XKSA1
Diode D_1&D_2	IDP30E65D2XKSA1

makes them inappropriate in renewable energy systems. In all, among the benchmarked topologies, the proposed converter can achieve superior performances (i.e., continuous input current, high voltage-gain, and wide duty-cycle control range).

Furthermore, the voltage stress across the capacitors, diodes, and switches among Y-source, quasi-Y-source and the proposed converter is compared by setting the winding factor to five, which is summarized in Table II. According to Table II, the voltage stresses of the capacitors among the proposed topology, Y-source and quasi-Y-source converter are very close, which means that the capacitor voltage stress is not affected by changing the position of the active switch. In addition, the voltage stresses over the diodes and switch in the proposed topology are significantly reduced. That is when a large voltage gain is needed, the proposed modified Y-source converter. This is beneficial to the device selection for high dc output voltages, thus, minimizing the cost.

III. EXPERIMENTAL VERIFICATION

A 250-W experimental prototype is built to verify the theoretical analysis.

The parameters of the prototype are listed in Table III. For the coupled-inductor, the windings are designed with 20, 12, and 20 turns in an interleaved structure to minimize the leakage inductance. The winding factor K is 5 and duty cycle is chosen as 0.6 to achieve a voltage gain of 10 for the proposed converter. A commercial dc source (ITECH IT6522 C DC Power Supply) was used in the experiments, and the converter supplied a passive load. Experimental results are shown in Fig. 5. The control and modulation were implemented in a digital signal processor (TMS320F28335).

As it is shown in Fig. 5(a), the output voltage V_o under the open-loop control is about 390 V, which matches the expected

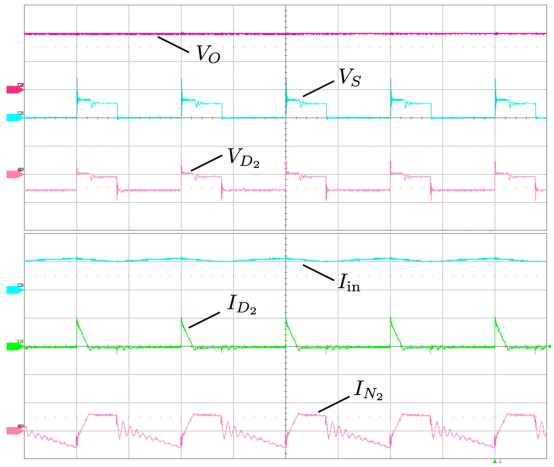

Fig. 5. Experimental results of the proposed converter operating at 200 W (output voltage V_o [200 V/div], switch voltage V_S [200 V/div], voltage of D_2 V_{D_2} [200 V/div], input current I_{in} [5 A/div], current of D_2 I_{D_2} [10 A/div], secondary current I_{N_2} [10 A/div], time [5 μs/div]).

theoretical value–400 V. Moreover, observations in Fig. 5(a) indicate that the input current I_{in} is continuous with low ripples and the mean value is about 5.4 A, meaning that the proposed converter draws a continuous current from the dc input. Therefore, the continuous input current and high voltage gain make the proposed Y-source converter more suitable for renewable energy applications, where a large conversion ratio is required. Moreover, it can be seen in Fig. 5(a) that the current flowing in the secondary winding of the coupled-inductor is a periodic signal without dc currents. This is because the capacitor C_1 in series with the coupled-inductor winding can prevent the magnetic core saturation.

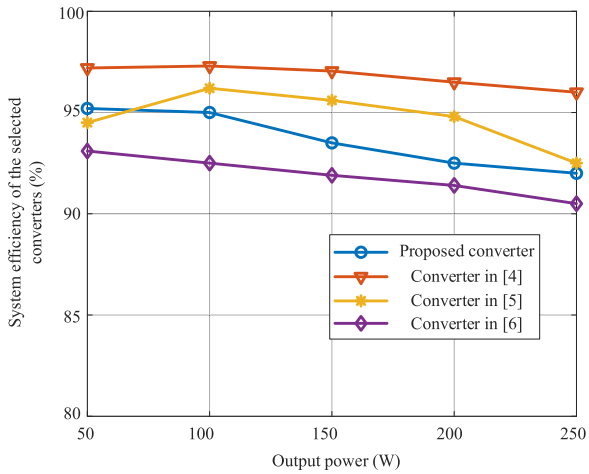

Fig. 6. Efficiency comparison of the selected dc–dc converters.

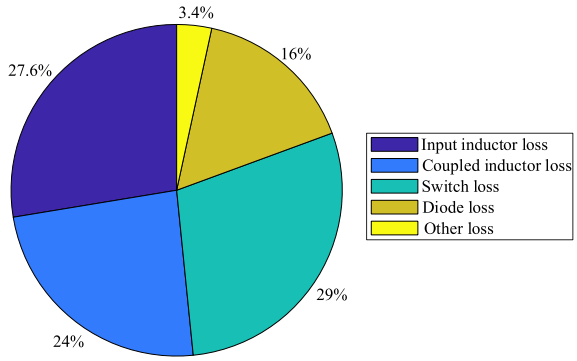

Fig. 7. Power loss distribution of the modified Y-source dc–dc converter.

More importantly, the voltage stress V_S over the active switch S is 110 V, which is much lower than the output voltage. Especially, the voltage spike shown in Fig. 5(b) is lower than the output voltage. This is in agreement with the previous analysis that the voltage stress of the active switch is significantly reduced compared with other Y-source converters. Similarly, the voltage V_{D_2} across the diode D_2 is about 110 V. As for the diode current I_{D_2}, it decreases from its maximum to zero during the turn-OFF state. Therefore, D_2 is working under the zero current switching (ZCS), which is beneficial to the converter efficiency.

Additionally, the efficiency of the proposed topology is measured with a high precision power analyzer (PPA5530). The efficiency of the converter under various loading conditions is shown in Fig. 6. The output power varies from 50 to 250 W for a constant input voltage (i.e., 40 V). It can be observed in Fig. 6 that the overall efficiency of the converter is above 92% at the rated power of 250 W and the peak efficiency is 95.2%. Notably, as compared in Fig. 6 the dc–dc converters in [4], [5] have a better efficiency, but both utilize more components than the proposed converter, leading to an increased cost. Moreover, it should be pointed out that the converter in [4] requires an LC filter in its input to limit the high frequency current ripples. Although more components are used in [6], its efficiency is lower than the proposed converter when the voltage gain is 10.

In addition, as shown in Fig. 7, the coupled-inductor and the input inductor account for a large proportion of the total losses of the proposed converter. Thus, the optimization of the proposed converter and the application of efficient power devices (e.g., gallium nitride devices) as the main active switch may also contribute to the efficiency improvement, which will be future work.

IV. Conclusion

In this letter, a modified Y-source dc–dc converter with a high voltage-gain has been proposed. The high voltage-gain can be flexibly achieved by setting the proper turns ratio of the coupled-inductor. Moreover, the proposed converter has a wide adjustable range of the duty cycle and it can draw a continuous current from the input source. One key feature of the proposed converter is that the voltage stress on the active switch is much lower compared with its counterparts. This allows the adoption of low power rating devices (e.g., gallium nitride devices) for high-voltage inverter applications, while maintaining low costs. Experimental tests have validated the effectiveness of the proposed dc–dc converter.

References

[1] Y. P. Siwakoti, F. Z. Peng, F. Blaabjerg, P. C. Loh, and G. E. Town, "Impedance-source networks for electric power conversion part I: A topological review," *IEEE Trans. Power Electron.*, vol. 30, no. 2, pp. 699–716, Feb. 2015.

[2] M. H. B. Nozadian, E. Babaei, S. H. Hosseini, and E. Shokati Asl, "Switched Z-source networks: A review," *IET Power Electron.*, vol. 12, no. 7, pp. 1616–1633, Jul. 2019.

[3] F. M. Shahir, E. Babaei, and M. Farsadi, "Extended topology for a boost DC-DC converter," *IEEE Trans. Power Electron.*, vol. 34, no. 3, pp. 2375–2384, Mar. 2019.

[4] L. Schmitz, R. F. Coelho, and D. C. Martins, "High step-up high efficiency DC-DC converter for module-integrated photovoltaic applications," in *Proc. 13th Brazilian Power Electron. Conf. 1st Southern Power Electron. Conf.*, Nov. 2015.

[5] R. Moradpour, H. Ardi, and A. Tavakoli, "Design and implementation of a new SEPIC-based high step-up DC/DC converter for renewable energy applications," *IEEE Trans. Ind. Electron.*, vol. 65, no. 2, pp. 1290–1297, Feb. 2018.

[6] Y. Tang, D. Fu, T. Wang, and Z. Xu, "Hybrid switched-inductor converters for high step-up conversion," *IEEE Trans. Ind. Electron.*, vol. 62, no. 3, pp. 1480–1490, Mar. 2015.

[7] F. Z. Peng, "Z-source inverter," *IEEE Trans. Ind. Appl.*, vol. 39, no. 2, pp. 504–510, Mar. 2003.

[8] P. C. Loh, D. Li, and F. Blaabjerg, "Γ-Z-source inverters," *IEEE Trans. Power Electron.*, vol. 28, no. 11, pp. 4880–4884, Nov. 2013.

[9] W. Mo, P. C. Loh, and F. Blaabjerg, "Asymmetrical Γ-source inverters," *IEEE Trans. Ind. Electron.*, vol. 61, no. 2, pp. 637–647, Feb. 2014.

[10] Y. P. Siwakoti, P. C. Loh, F. Blaabjerg, and G. E. Town, "Y-source impedance network," *IEEE Trans. Power Electron.*, vol. 29, no. 7, pp. 3250–3254, Jul. 2014.

[11] Y. P. Siwakoti, F. Blaabjerg, and P. C. Loh, "Quasi-Y-source boost DC-DC converter," *IEEE Trans. Power Electron.*, vol. 30, no. 12, pp. 6514–6519, Dec. 2015.

[12] Y. Wang *et al.*, "A family of Y-source DC/DC converter based on switched inductor," *IEEE Trans. Ind. Appl.*, vol. 55, no. 2, pp. 1587–1597, Mar. 2019.

[13] M. Nguyen, Y. Lim, J. Choi, and Y. Choi, "Trans-switched boost inverters," *IET Power Electron.*, vol. 9, no. 5, pp. 1065–1073, 2016.

[14] S. S. Nag and S. Mishra, "A coupled inductor based high boost inverter with sub-unity turns-ratio range," *IEEE Trans. Power Electron.*, vol. 31, no. 11, pp. 7534–7543, Nov. 2016.

[15] A. R. Majarshin and E. Babaei, "High step-up DC-DC converter with reduced voltage and current stress of elements," *IET Power Electron.* vol. 12, no. 11, pp. 2884–2894, Sep. 2019.